ACCEPTED VERSION

Sebastian W. S. Ng, David G. Lancaster, Tanya M. Monro, Peter C. Henry, and David J. Ottaway

Air-clad holmium-doped silica fiber laser

IEEE Journal of Quantum Electronics, 2016; 52(2):1600108-1-1600108-8

© 2015 IEEE. Personal use of this material is permitted. Permission from IEEE must be obtained for all other uses, in any current or future media, including reprinting/republishing this material for advertising or promotional purposes, creating new collective works, for resale or redistribution to servers or lists, or reuse of any copyrighted component of this work in other works.

Published version at: http://dx.doi.org/10.1109/JQE.2015.2507518

PERMISSIONS

http://www.ieee.org/publications_standards/publications/rights/rights_policies.html

Authors and/or their employers shall have the right to post the accepted version of IEEE-copyrighted articles on their own personal servers or the servers of their institutions or employers without permission from IEEE, provided that the posted version includes a prominently displayed IEEE copyright notice (as shown in 8.1.9.B, above) and, when published, a full citation to the original IEEE publication, including a Digital Object Identifier (DOI). Authors shall not post the final, published versions of their articles.

14 December 2016

http://hdl.handle.net/2440/100300

Air-clad holmium-doped silica fiber laser

Sebastian W. S. Ng, David G. Lancaster, Tanya M. Monro, Peter Henry, and David J. Ottaway

***Abstract*—We report the design, fabrication and operation of an air-clad holmium-doped fiber laser that was manufactured by directly milling the rare-earth doped preform. This silica fiber laser operates at 2.1 µm with a slope efficiency of 49.7 %, and is in-band pumped with a 1.94 µm thulium fiber laser. To the best of our knowledge this is the first demonstration of an air-clad holmium-doped fiber laser.**

***Index Terms*—fiber laser, double-clad fiber, holmium.**

I. Introduction

HIGH beam quality holmium emission at 2.1 µm can be efficiently transmitted through the atmosphere and converted to mid-infrared with low loss. Silica has become the standard host due to its high mechanical strength and melting point which are essential for high power fiber laser operation. Its infrared vibrational absorption results in significant attenuation above 2.1 µm [1] meaning that holmium is the longest wavelength rare-earth emission that silica can support.

Fiber lasers operating at 2.1 µm offer a fourfold increase in core area while maintaining single mode confinement compared to ytterbium-doped fiber lasers operating around 1 µm reducing the core intensity for the same circulating power. This is significant as power scaling of robustly single-mode rare-earth fiber lasers can be limited by the onset of stimulated Raman scattering in broadband lasers and Stimulated Brillouin Scattering (SBS) for narrow linewidth lasers [2]. The threshold for these non-linear effects increases with the intensity in the core and device length. This SBS limit is particularly relevant to third generation gravitational wave detectors where up to 250 Watts of extremely narrow-linewidth infrared-radiation is proposed at a wavelength between 1.5-2.1 µm to enable the use of thermally stable silicon optics [3].

Holmium may be pumped by conventional diodes at 1.15 µm [4] which results in a large quantum defect. In-band pumping by direct 1.9 µm excitation into the upper laser level ($_5I^7$ energy level) reduces the quantum defect, and hence heat load. Currently 1.9 µm diode lasers have limited output power but this is increasing and in the future they may provide a viable high-power low brightness pump source. Currently high-power thulium fiber lasers, optically pumped by 790 nm diodes, provide an alternative pump source which has high brightness but increased complexity [5]–[7]. The two common pumping regimes for holmium emission at 2.1 µm are shown in Fig. 1.

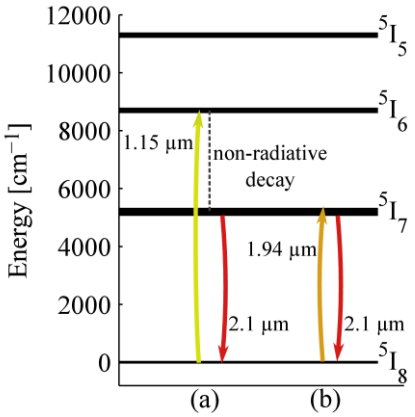

Fig. 1. Simplified energy level diagram of trivalent holmium ion showing transitions for (a) 1.15 µm, and (b) the in-band 1.94 µm pumping regime [8].

The efficiency of the 790 nm InGaAs pump diodes at 71 % [9] with the thulium-doped fiber lasers efficiency of around 60 % provides a combined efficiency of 43 % for a 1.95 µm pump source. Conversely InGaAsP diode lasers operating around 2 µm have been demonstrated with powers up to 100 W [10] and with efficiencies of up to 55 % [11], this potential improvement in overall efficiency combined with the simplified, laser design makes a directly diode pumped holmium fiber laser an attractive portable source where high beam quality 2.1 µm emission is desired.

Double-clad fiber designs, allow an increase in the NA for optical pumping that is essential for the efficient pumping of fiber lasers by lower brightness pump diodes. For shorter wavelengths these fibers typically use low index polymers for their outer-cladding. However, these polymers display non-negligible absorption at 1.9 µm [12] leading to a significant drop in device efficiency and limited power scaling because these polymers have a relatively low thermal failure limit compared to silica. For this reason there has been significant interest in alternative outer-cladding structures for high power ytterbium fiber lasers [13], [14].

The primary alternatives to polymer claddings are highly fluorine-doped silica outer-cladding and air-clad fiber. The

Manuscript received September 24, 2015. This work was supported in part by the Asian Office of Aerospace Research and Development (AOARD - AFOSR), grant # 144033 and through the Premier's Science and Research Fund, South Australia. T. M. Monro acknowledges the support of an ARC Georgina Sweet Laureate Fellowship. S. W. S. Ng and D. J. Ottaway are with the Department of Physics, University of Adelaide, Adelaide, SA 5005 Australia (e-mail: sebastian.ng@adelaide.edu.au; david.ottaway@adelaide.edu.au).

D. G. Lancaster, P. Henry and T. M. Monro were with the University of Adelaide, SA 5005 Australia. D. G. Lancaster and T. M. Monro are now with Laser Physics and Photonic Devices Laboratories, The University of South Australia, Adelaide, SA 5000, Australia (e-mail: david.lancaster@unisa.edu.au; tanya.monro@unisa.edu.au). P. Henry is now at MG Scientific Glassblowing, Newtown, NSW 2042, Australia (e-mail: mgsciglass@optusnet.com.au).

xxxx–xxxx/xx © 2015 IEEE

former can be fabricated by over-jacketing silica preforms with commercially available fluorine-doped silica tubes and can achieve cladding numerical apertures (NAs) of 0.28 [14]. NAs of 0.3 have been demonstrated with a combination of outside-vapor-deposition and increasing the inner cladding refractive index by doping with Germanium [15] Holmium-doped core, fluorine-doped outer-claddings have been demonstrated with output powers up to 400 W [16]. Higher NAs up to 0.9 have been demonstrated with air-cladding solid cores at shorter wavelengths [17] and have been demonstrated with powers in the kW level [18]. Air cladding is conventionally formed using a capillary stacking technique that is ideal for long fiber lengths and established fiber designs. The stack and draw technique is capable of producing air-cladding with very large numbers of holes and is compatible with photonic crystal guiding feature where a large number of air holes are used to provide guidance to the core of the fiber allowing single mode performance with large cores [17], [18]. However, many holed fibers are not always required. Ultrasonic milling of a silica rod [19] provides a more flexible air-cladding and directly milling the rare-earth-doped preform reduces the complexity required to fabricate an air-clad RE-doped fiber.

The transition from core-pumped to cladding-pumped fiber laser designs achieves a significant increase in pump power that can be coupled into the fiber. The introduction of double-clad architectures in thulium-doped fibers resulted in a fourfold increase in output powers at the time [20] and single mode output powers have continued to increase significantly [21]. However, the double-cladding architecture results in reduced pump absorption for a fixed core size and hence longer devices. The length of holmium-doped fibers that can be used for efficient high-power applications is limited due to the background silica loss at 2.1 µm, and the onset of non-linear effects [1], [2]. Pump absorption for an efficient fiber laser design cannot be raised by increasing the dopant concentration because ion-clustering impacts efficiency [22]. Hence, a low cladding-to-core ratio, high NA clad architecture is predicted to allow a beneficial trade-off between efficiency and power scaling, while providing a pathway for the use of low brightness pump sources.

This paper presents the first demonstration of a double-clad, air-clad holmium-doped fiber laser that utilizes the in-band core pumping regime and cladding-to-core geometry discussed. The preform is produced from a modified chemical vapor deposition (MCVD) fabricated preform with the preform directly milled to form the air-cladding.

II. Fiber Manufacture

A 7-hole air-clad holmium-doped silica fiber was produced by fabricating a step-index holmium core-doped preform inside a high purity F300 silica deposition tube using the MCVD process. The core was solution-doped with a high aluminum chloride to holmium ratio to achieve an increased index core. The alumino-silicate core is well known to improve rare-earth ion solubility, and thus reduce clustering of the holmium ions that can compromise efficiency [22]. The strongly guiding core, with a NA~0.13 estimated from the refractive index profile, was chosen to allow characterization of the new fiber geometry without significant bend-induced core confinement loss. The refractive index profile of the preform is shown in Fig. 2, with an inset schematic of the fiber geometry. The preform was over-jacketed to increase the fiber diameter for structural stability and ease of handling.

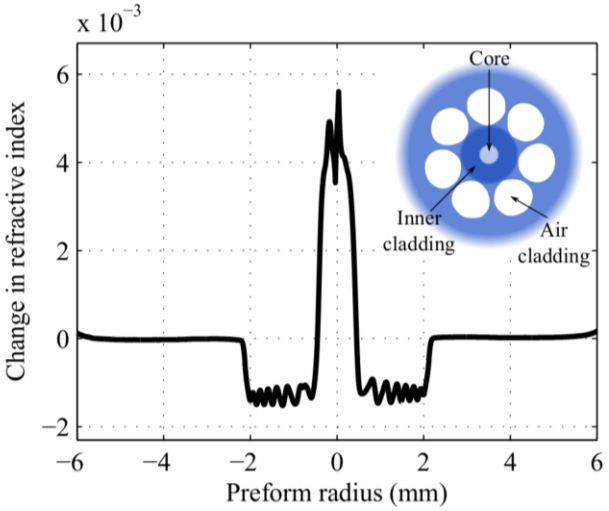

Fig. 2. Holmium-doped preform refractive index profile. The deposited region of glass between -2 and 2 mm form the inner cladding of the air-clad fiber. Inset: Fiber schematic with air cladding.

A 100 mm length of the preform was ultra-sonically milled to achieve a 7-hole structure surrounding the core using a 2.8 mm diameter hollow drill bit (1 mm/min feed-rate) and a 20 kHz ultrasonic frequency (Sonic-Mill™ S10 ultrasonic mill). The holes were centered on an 8 mm diameter ring around the core, to closely surround the ultra-pure MCVD deposited glass which formed the inner-cladding. This maintained a uniform density of glass surrounding the holes which prevented uneven expansion during fiber drawing and limited the pump-guiding region of the inner-cladding to the high purity, low water content deposition layers. A high purity cladding is required to limit the effect of OH absorption in silica at the 1.94 µm pump wavelength [23]. The thickness of the deposited glass was tailored for a low core to inner-cladding area ratio to increase pump absorption and reduce device length. The cross-section of the drilled preform is shown in Fig. 3.

Fig. 3. Cross-section of the over-jacketed and drilled holmium-doped preform, showing the pink holmium-doped core and the refractive index variations of the deposited silica of the inner-cladding surrounded by the 7 air-holes.

The fiber was drawn using active pressurization of the air-cladding holes to control the expansion of the holes. This was achieved by pressurizing a glass tube fused to the top of the drilled preform. The fiber was drawn in three stages by increasing internal pressure and evaluating the cross-section of the fiber up to 1.5 kPa. Further increases in pressure resulted in unstable expansion of the holes resulting in non-symmetric fiber cross-sections. The highest stable internal pressures resulted in a fiber with a core diameter of 10 µm, an inner cladding diameter of approximately 45 µm, and an outer diameter of 288 µm as shown in Fig. 4. The resultant core diameter provides a V-number of 2.04 this should provide single mode laser performance. The thickness of the struts at their narrowest points was ~1 µm. The fiber was found to have acceptable mechanical strength however reproducible cleaves proved difficult to achieve. Analysis of the fiber cross-section indicates a 24 % reduction in the second moment of area compared to a solid fiber, predicting a non-negligible reduction in mechanical stability. The variation in the second moment of area in the orthogonal axes of the cross-section indicated a variation of less than a percent, consistent with our practical handling of the fiber which showed no significant preference to the orientation of failure. This suggests that the size and position rather than the number of holes may be varied to improve mechanical durability. This reduction in mechanical stability would most easily be improved by increasing the thickness of the over-jacketed region. For direct milling this is advantageous as additional holes significantly increase fabrication time.

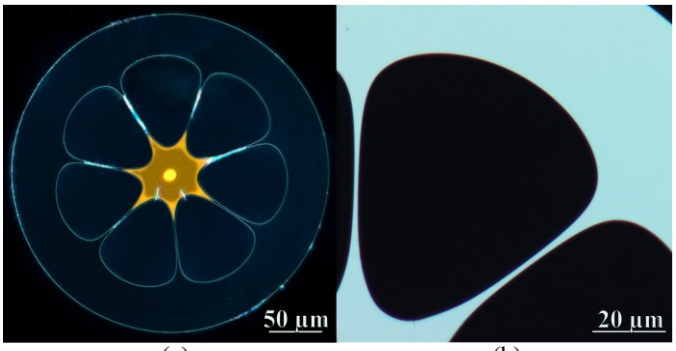

Fig. 4. (a) A dark field microscope image of the air-clad fiber with core and inner-cladding illuminated in transmission and (b) microscope image of the air-cladding struts.

Direct milling of the preform offers reduced complexity for simple, low yield microstructured fibers as the required structure may be machined into the preform, straight from the MCVD lathe, with relative freedom.

III. Fiber Characterization

Attenuation measurements were performed by probing the inner-cladding of the air-clad fiber with a thulium-doped fiber laser operating at 1945 nm. Attenuation at this wavelength was measured to be 0.85 dB/m, this was below our desired pump absorption and was due to insufficient uptake of holmium during the solution doping phase. This reduced absorption will result in a longer device length and as such reduced efficiency. In order to determine the water content in the fiber a supercontinuum source was used to evaluate the 1.4 µm hydroxyl overtone resulting in 0.1 dB/m for both the cladding and the core. This level of OH contamination is likely to have a moderate effect on the lasing efficiency at increasing lengths.

The NA of three sections of fiber, each drawn with increasing internal gas pressure, were measured using a 1.53 µm source with the measured NA shown in Fig. 5. The NA increases to 0.42 with decreasing strut thickness. Unlike fluorine-doped cladding [24] the NA for air-clad fiber increases with wavelength due to the reduction of the relative thickness of the struts to the wavelength. To estimate the improvement at 1.95 µm, the 1.53 µm fiber source was replaced with a supercontinuum filtered with an acousto-optical tunable filter. The NA was found to increase from 0.32 at 1.25 µm to 0.4 at 1.7 µm and then flatten off as 2 µm was approached. Although significantly lower than the record numerical apertures for air-clad fibers of 0.9, these measured NAs, as shown in Fig. 6, provide a significant improvement over the NAs demonstrated at shorter wavelengths with fluorine-doped cladding [14].

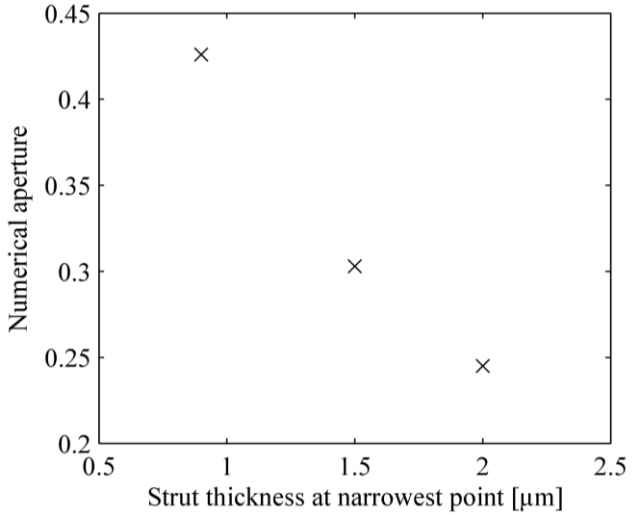

Fig. 5. The NA, measured at 1.53 µm, versus the strut thickness of the air-cladding at their narrowest points.

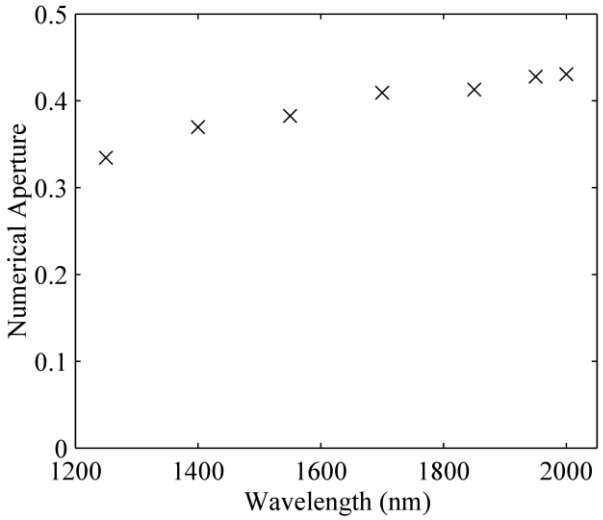

Fig. 6. NA versus wavelength using a supercontinuum source filtered with an AOTF. This confirms an increasing NA with wavelength.

IV. Laser Performance

Laser performance of the fiber was characterized in a double-pass pump configuration shown in Fig. 7. Although significantly brighter than 1.9 µm diodes, a double-clad thulium fiber laser with M^2~3 operating at the 1.95 µm holmium absorption peak was used to demonstrate the air-clad fiber performance due to its availability. The coincident input and output beam paths were chosen due to thermal failure of the coatings of the input dichroic when butt coupled to the input fiber facet.

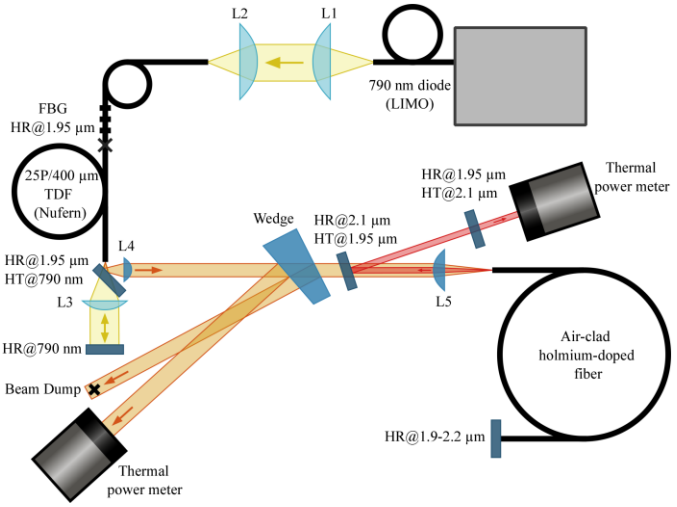

Fig. 7. Laser characterization apparatus with a fiber Bragg grating (FBG) stabilized, 790 nm diode-pumped thulium-doped fiber laser providing the 1945 nm pump power for the holmium-doped air-clad fiber in a single-ended pump and collection configuration. L1,L2 are ThorLabs Al5040-B and L3 is a ThorLabs Al3026-B aspheric lens. L4 and L5 are Edmund Optics L-BAL35 Aspheric lenses with Altechna 2 µm AR coatings with 22.6 mm and 15 mm focal lengths respectively.

The pump power was monitored and calibrated using the front face reflection of a wedge in the collimated beam. An f=22.6 mm lens was used to collimate the pump beam, which was then launched into the inner-cladding of the fiber by an f=15 mm aspheric lens AR coated at 2 µm. The laser cavity was formed between the Fresnel reflection of the input fiber facet and a butt-coupled broadband high reflection (HR) dichroic at 1.9-2.2 µm. The laser output was separated from the input pump beam using a 10° angled dichroic filter with high transmission (HT) at 1.95 µm, HR at 2.15 µm. The transmission of the optical elements in the output beam path were measured using an Agilent Cary 5000 UV-VIS-NIR spectrometer as a function of wavelength and incidence angle to allow calibration of the output power to the poor performance of the available optics.

The lasing performance versus fiber length is shown in Fig. 8. The emission wavelength was measured with a Yokogawa AQ6375 OSA with a typical output spectrum shown in Fig. 9. The output spectra were measured for each length, shown in Fig. 10. As the cavity length increases the laser output redshifts and then approaches 2.1 µm for fibers longer than 8 m. This corresponds to the peak efficiency of the laser cutback from Fig. 8 demonstrating adequate gain at the desired emission of 2.1 µm. The transmission of the output beam path was used to calibrate the output for each length with transmission ranging from 88-93 %. Significant scatter in the slope efficiency is due to large variation in the quality of the fiber cleave facets. In this configuration the maximum slope efficiency was 49.7 % with a 770 mW threshold for an 8.75 m resonator length. This efficiency is below the record efficiency of 62 % achieved in a 4 m double-clad holmium fiber laser by reducing OH concentration [25]. The reduction in efficiency is due to increased absorption of the lasing emission from the intrinsic silica multiphonon absorption edge, higher OH-concentration and longer cavity length.

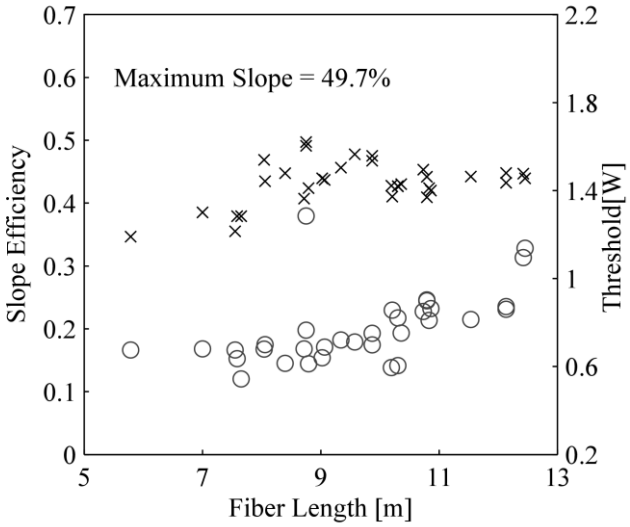

Fig. 8. Lasing threshold (circles) and slope efficiency (crosses) versus the length of the fiber.

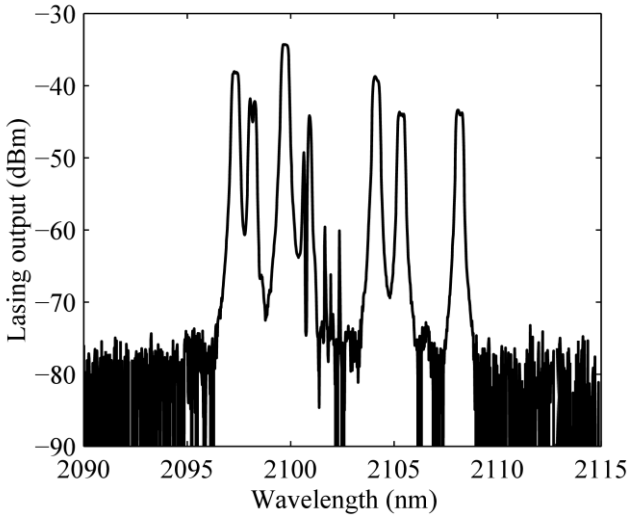

Fig. 9. A typical fiber laser output spectra from the air-clad fiber laser.

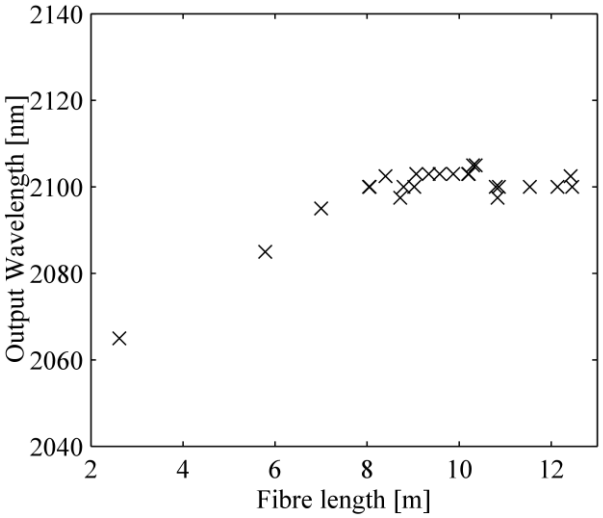

Fig. 10. The central output wavelength versus fiber length. The crosses indicate the central position of the spectra and had widths of around 10 nm.

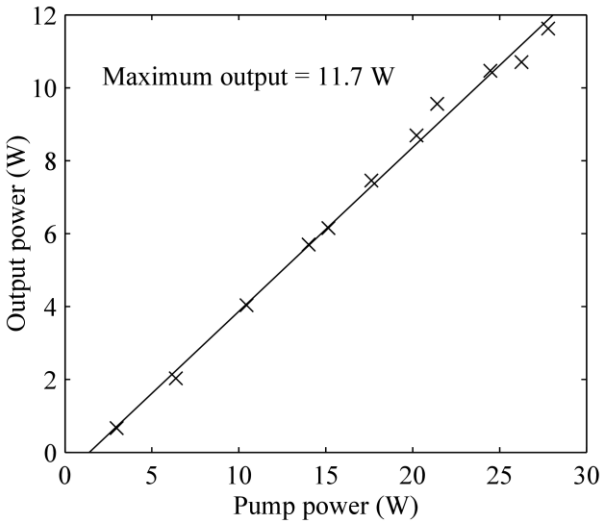

Fig. 11. The output power of the air-clad holmium fiber laser versus the pump power incident on the fiber. Pump-coupling was optimized throughout the measurement to overcome thermal lensing in the coupling optics. This bulk optic thermal lensing resulted in the increase of scatter above 20 W of incident pump power.

A maximum output of 11.7 W shown in Fig. 11. Efficiency roll-off was observed after ~20 W incident pump. This was due to combined pump and signal absorption in the coupling optics resulting in thermal lensing and a reduction of pump coupling. To partially overcome the thermal lensing the input coupling was manually optimized with increasing pump power.

The collimated fiber laser output was imaged with a pyroelectric camera (Ophir Pyrocam III). While the beam appears to be single transverse mode, slight illumination was observed in the star-shaped inner-cladding as shown in Fig. 12. To determine the effect of this cladding light on the beam quality, beam-quality measurements were performed. The reflection of the output beam from an uncoated wedge was passed through an uncoated f=1000 mm plano-convex lens and focused on the array of the pyroelectric camera. The background intensity of the camera was calibrated and the D4σ diameter of the focus was estimated along the beam length. A M^2 fit of 1.3 was achieved from the resultant beam diameters as shown in Fig. 13. This also indicated some astigmatism in the output beam which is consistent with the slightly distorted core seen in Fig. 4. An aperture was applied to the collimated output beam which reduced the output power by 1 %; the M^2 was then measured to be 1.2. This indicates that in this configuration the narrow high NA cladding does not promote parasitic cladding modes and the scattered emission does not significantly impact the beam quality. The reduction in M^2 from 1 expected from a step index fiber with a V-number of less than 2.4 is contributed to aberrations from the path of the output beam.

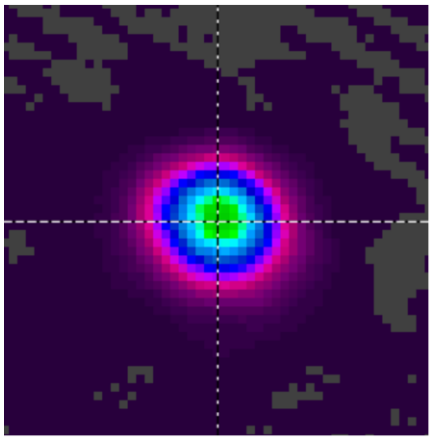

Fig. 12. The near-field beam profile of the laser output.

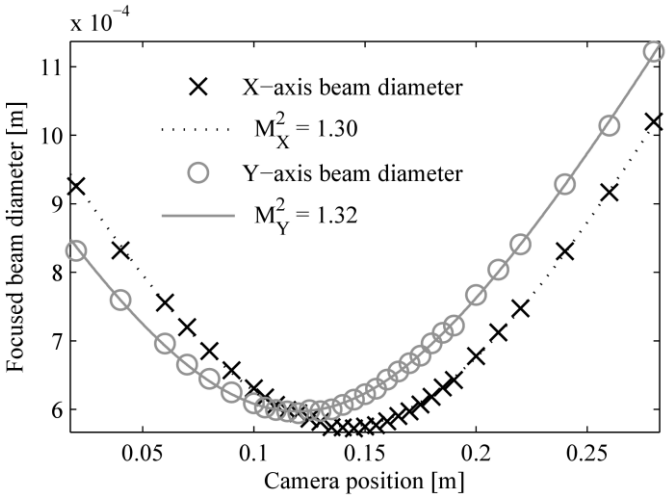

Fig. 13. The beam diameter through the focal point of the measurement showing a fit to M^2 of 1.30±0.01 along the X-axis and 1.32±0.01 along the Y-axis with the uncertainty ranges indicating the 95% confidence intervals for the fit. The D4σ beam diameter was measured along the beam direction on a pyroelectric camera.

However, this cladding-light is expected to become more of a problem at higher power levels and lower NA cores and is the subject of further investigation.

V. Thermal Modelling

Previous studies into air-clad laser structures have indicated that internal convection does not play a significant role in the transfer of heat from a rare-earth-doped core because of the small hole sizes in MOFs [26]. Conventional air-clad fibers rely

on a large number of very small holes, ideal for conductive transfer across the holey cladding. In order to maximize the NA significant expansion of the air holes was required with the limited number of holes used, resulting in long thin struts and large air cavities. To determine the effect of these larger air holes, and to understand their impact on heat conduction, a 2D coupled convection and conduction FEM analysis was performed.

The measured fiber geometry was imported into the model including core diameter, air-holes, and acrylate coating. To simulate the thermal conditions of the fiber laser, a conservative 5 W/m heat load to simulate the non-linear absorption of pump power was applied to the core, the left perimeter of the acrylate was set to ambient temperature to emulate perfect conductive cooling to a spool, and the right perimeter was set as a thermal insulator. The results are shown in Fig. 14 which shows a rise in the peak core temperature from the surroundings of 17.5 K. The total heat-flux through the fiber was evaluated and although convective cells are predicted to form within the air holes a maximum velocity of $3.8\text{x}10^{-7}$ m/s is shown in Fig. 15, the heat flux was found to be insignificant through the air holes compared to the struts consistent with the small air holes in previous analyses. The configuration was then simulated without convection and no significant temperature variation was observed between the two models.

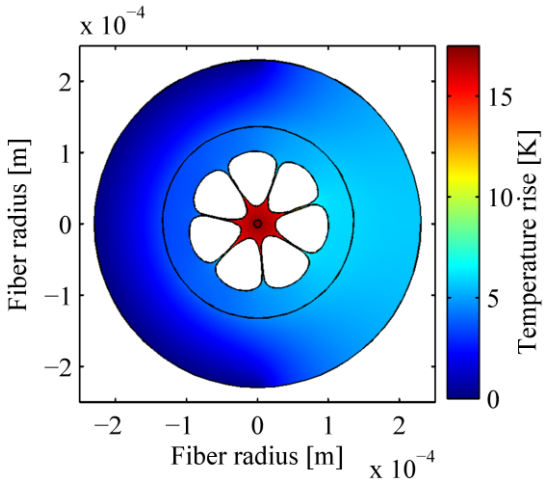

Fig. 14. Finite element modelling of the temperature cross-section of air-clad fiber at 5 W/m heat load in the core with the left perimeter conducting to ambient temperature and the right perimeter thermally insulated to simulate cooling on a fiber spool.

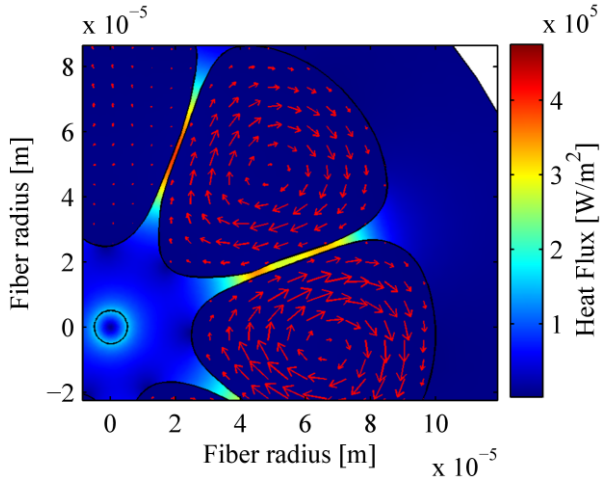

Fig. 15. A close-up of the modelled outward heat flux through the fiber and the velocity field (arrows) of the convection in the air holes with a maximum velocity of $3.7\text{x}10^{-7}$ m/s.

To evaluate the potential for power scaling of this fiber the maximum temperature was evaluated from 1-20 W/m thermal load shown in Fig. 16. The simple conduction-only FEM analysis was performed comparing the air-clad fiber with a solid fiber of equal diameter. The air-clad fiber was compared to a solid glass fiber of equal diameter and each were simulated in the spool-cooled configuration described and also without the acrylate-clad, setting the exterior of the glass cladding to ambient temperature.

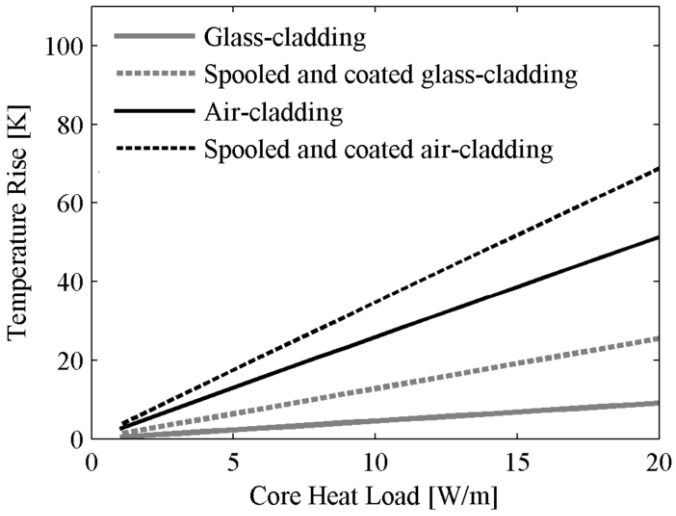

Fig. 16. Thermal simulation of the rise in temperature in core versus heat load in the core for air-clad (black) and solid fiber of equal diameter (Grey) each with bare glass cladding (solid) and acrylate coatings with spool-cooling (dashed).

The rise in maximum core temperature predicts the thermal insulation due to the air-cladding to be much more significant than that of the acrylate cladding. With a 5 W/m heat load near the input of the fiber the solid fiber is predicted to have a 4 K temperature rise due to the spool-cooled acrylate coating and a 10 K temperature rise due to the addition of air holes alone. This relatively small temperature rise in the sort section of fiber near the input is not expected to have a significant impact on the lasing efficiency. The rate that the temperature rise from the bare conduction cooled fiber increases with heat load is

consistent between the solid and air-clad fiber, suggesting the struts provide no additional thermal penalty due to their spacing. Extension of this modelling predicts the fiber core will reach glass transition temperature at a core heat load of around 400 W/m. However, as the temperature in the core rises the efficiency is expected to decrease as the ground state ($^5I_8$ energy band) populate the upper levels of the band red shifting the energy transfer further into the 2.2 µm absorption peak. With the efficiencies demonstrated above and the simplified boundary conditions an upper limit on the achievable powers with this fiber is set around 1.2 kW. This is limited by the thermal heating of the fiber core near the input, but is significantly above the currently available 2 µm pump diode power levels.

VI. Discussion & Conclusion

Ytterbium, erbium and thulium fiber lasers predominantly rely on diode-pumped configurations for efficient and cost effective systems. These lasers are pumped in the near-infrared hence allow the use of polymer claddings providing NAs of around 0.4 for brightness conversion. Due to the strong polymer absorption at 2 µm, holmium fiber lasers will either require a large quantum defect by relying on 1.15 µm pumping or the reduced pump acceptance of fluorine-doped claddings, or the thermal and structural limitations of air-clad fibers. The fiber presented forms a proof of principle demonstration of future air-clad holmium fiber lasers and as such provides many avenues for further optimization in efficiency, heat transfer, and pump acceptance.

Although the direct milling method presented here reduces the number of process steps compared to the stack and draw technique it required a significant time investment with a single 7-hole preform required on the order of 12 hours to drill. However, since the production of this preform the drilling times have decreased by an order of magnitude (10 mm/min for 2.8 mm holes) with the use of advanced CNC machining. Additionally, minimum drill sizes of 0.5 mm are achievable enabling greater flexibility of hole size, albeit at slower feed rates and shorter lengths.

The efficiency demonstrated with the low core-to-cladding ratio was limited by device length related losses. The low concentration was due to a reduced uptake of holmium dopant in the unfused core during preform manufacture and is below that required to prevent losses due to ion-clustering. This was combined with the relatively large OH concentration of around 2 ppm compared to the concentrations achieved for the record slope efficiencies. There is also significant scope for the improvement of pump acceptance and an improvement to heat transfer through an increase in the number of cladding holes allowing smaller air holes and narrower struts.

Hanson, et al. [27] suggested that the optimal air-clad NAs are 0.55 to 0.65 as the handling and cleavability of conventional air-clad fibers becomes a problem providing an upper limit on the practicality of air-cladding NAs. However, these observations were made in relation to 1 µm ytterbium lasers with strut-to-wavelength ratios of around 0.5. For 1.94 µm pump confinement these NAs should be achieved with around twice the strut thickness. As the struts provide the dominant mechanism for heat transfer this should provide a significant increase in the thermal load limit or alternatively allow significant improvements to maximum practical NAs. Comparing these observations to the NAs investigated by Wadsworth et al. [17] practical pump claddings of above 0.8 should be achievable. These optimizations present air-clad holmium lasers as an attractive option for the future development of in-band, cladding-pumped holmium fiber lasers as the availability of high power 1.94 µm diode lasers improves and particularly for narrow linewidth applications where SBS sets strict limitations on device length. The combination of an improved NA promoting simplified device design and the potential for improved device efficiency provide holmium-doped air-clad fiber lasers as a strong candidate for portable high beam quality 2.1 µm sources.

We have demonstrated, to the best of our knowledge, the first holmium-doped air-clad silica fiber laser and achieved a slope efficiency of 49.7 % and output power of 11.7 W.

Acknowledgment

The authors would like to acknowledge Roman Kostecki for the preform milling.

References

[1] A. S. Kurkov, E. M. Sholokhov, V. B. Tsvetkov, V. Marakulin, L. Minashina, O. I. Medvedkov, and F. Kosolapov, “Holmium fibre laser with record quantum efficiency,” *IEEE J. Quantum Electron.*, 41(6), 492-494, 2011.

[2] J. W. Dawson, M. J. Messerly, R. J. Beach, M. Y. Shverdin, E. Stappaerts, A. K. Sridharan, P. H. Pax, J. E. Heebner, C. W. Siders, and C. P. J. Barty, “Analysis of the scalability of diffraction-limited fiber lasers and amplifiers to high average power,” *Opt. Exp.*, 16(17), 13240-66, 2008.

[3] D. McClelland, M. Evans, B. Lantz, I. Martin, V. Quetschke, and R. Schnabel, (2015, December 12) “Instrument Science White Paper 2015”, *LIGO Scientific Collaboration*, LIGO-T1500290-v2, [Online]. Available: https://dcc.ligo.org/LIGO-T1500290/public

[4] S. D. Jackson, F. Bugge, and G. Erbert, “Directly diode-pumped holmium fibre lasers,” *Opt. Lett.*, 32(17), 2496-8, 2007.

[5] S. D. Jackson, “Mid-infrared Holmium Fiber Lasers”, *IEEE J. of Quantum Electron*, 42(2), 187-191, 2006.

[6] K. S. Wu, D. Ottaway, J. Munch, D. G. Lancaster, S. Bennetts, and S. D. Jackson, “Gain-switched holmium-doped fibre laser,” *Opt. Exp.*, 17(23), 20872-7, 2009.

[7] S. Hollitt, N. Simakov, A. Hemming, J. Haub, and A. Carter, “A linearly polarised, pulsed Ho-doped fiber laser,” *Opt. Exp.*, 20(15), 16285-16290, 2012.

[8] J. B. Gruber, M. E. Hills, M. D. Seltzer, S. B. Stevens, C. Morrison, G. Turner, and M. R. Kokta, “Energy levels and crystal quantum states of trivalent holmium in Yttrium aluminum garnet,” *J. of Appl. Phys.*, 69(12), 8183, 1991.

[9] P. Crump, W. Dong, M. Grimshaw, J. Wang, S. Patterson, D. Wise, M. DeFranza, S. Elim, S. Zhang, M. Bougher, J. Patterson, S. Das, J. Bell, J. Farmer, M. DeVito, and R. Martinsen, "100-W+ diode laser bars show > 71% power conversion from 790- nm to 1000-nm and have clear route to > 85%," *Proc. SPIE* Vol. 6456, pp. 22, 2007.

[10] X. He, D. Xu, A. Ovtchinnikov, F. Malarayap, R. Supe, S. Wilson, and R. Patel, "High power efficient GaInAsP/InP (1.9 µm) laser diode arrays," *Electron. Lett.,* 35, 397, 1999.

[11] J. S. Major Jr, D. W. Nam, J. S. Osinski, D. F. Welch, "High-power 2.0 µm InGaAsP laser diodes," *IEEE Photon. Technol. Lett.,* vol.5, no.6, pp.594-596, 1993

[12] M. Rahou, J. Andrews, and G. Rosengarten, "Experimental study of direct transfer of concentrated solar radiation through optical fibres to high temperature thermal applications," *Proc. SPIE* Vol. 9191, pp. 91910L, 2014.

[13] F. Stutzki, F. Jansen, T. Eidam, A. Steinmetz, C. Jauregui, J. Limpert, and A. Tünnermann, “High average power large-pitch fiber amplifier with robust single-mode operation,” *Opt. Lett.*, 36(5), 689-691, 2011.

[14] L. Dong, H. McKay, L. Fu, M. Ohta, A. Marcinkevicius, S. Suzuki, and M. E. Fermann, "Ytterbium-doped all glass leakage channel fibers with highly fluorine-doped silica pump cladding," *Opt. Exp.*, 17(11), 8962-9, 2009.
[15] J. Wang, D. T. Walton, and L. A. Zenteno. "All-glass high NA Yb-doped double-clad laser fibres made by outside-vapour deposition," *Electron. Lett.,* 40.10, 590-592, 2004.
[16] A. Hemming, N. Simakov, A. Davidson, S. Bennetts, M. Hughes, N. Carmody, P. Davies, L. Corena, D. Stepanov, J. Haub, R. Swain, and A. Carter, "A monolithic cladding pumped holmium-doped fibre laser," *Conf. Lasers and Electro-Optics Europe—Tech. Dig.*, 2013.
[17] W. Wadsworth, and R. Percival, "Very high numerical aperture fibers," *IEEE Photon. Tech. Lett.,* 16(3), 843-845, 2004.
[18] C. Wirth, O. Schmidt, A. Kliner, T. Schreiber, R. Eberhardt, and A. Tünnermann, "High-power tandem pumped fiber amplifier with an output power of 2.9 kW," *Opt. Lett.*, 36(16), 3061–3063, 2011.
[19] K. Mukasa, M. N. Petrovich, F. Poletti, A. Webb, J. Hayes, A. Van Brakel, R. A. Correa, L. Provost, J. Sahu, P. Petropoulos, and D. J. Richardson, "Novel fabrication method of highly-nonlinear silica holey fibres," *Conf. Lasers and Electro-Optics Europe—Tech. Dig*., 2006
[20] S. D. Jackson, and T. King, "High-power diode-cladding-pumped Tm-doped silica fiber laser," *Opt. Lett.,* 23, 1462–1464, 1998.
[21] G. D. Goodno, L. D. Book, and J. E. Rothenberg, "Single-mode 608 W thulium fiber amplifier," *Opt. Lett.,* 34, 1204–1206, 2009.
[22] A. S. Kurkov, E. M. Sholokhov, V. Marakulin, L.A. Minashina, "Effect of active-ion concentration on holmium fibre laser efficiency," *IEEE J. Quantum Electron.*, 40(5), 386-388, 2010.
[23] O. Humbach, H. Fabian, U. Grzesik, U. Haken, and W. Heitmann, "Analysis of OH absorption bands in synthetic silica," *J. of Non-Crystal. Solids,* 203, 19-26, 1996.
[24] J. W. Fleming, and D. L. Wood, "Refractive index dispersion and related properties in fluorine doped silica," *Applied Optics,* 22(19), 3102, 1983.
[25] E. J. Friebele, C. G. Askins, J. R. Peele, B. M. Wright, N. J. Condon, S. O'Connor, S. R. Bowman, "Ho-doped fiber for high energy laser applications," *Proc. SPIE* Vol. 8961, pp. 20, 2014.
[26] B. Zintzen, T. Langer, J. Geiger, D. Hoffmann, and P. Loosen, "Heat transport in solid and air-clad fibers for high-power fiber lasers," *Opt. Exp.*, 15(25), 16787–16793, 2007.
[27] K. P. Hansen, C. B. Olausson, J. Broeng, D. Noordegraaf, M. D. Maack, T. T. Alkeskjold, H. R. Simonsen, "Airclad fiber laser technology," *Optical Engineering*, 50(11), 111609, 2011.

Sebastian W.S. Ng completed a Bachelor of Science majoring in Experimental and Theoretical Physics with a Bachelor of Engineering majoring in Mechanical Engineering with first class honours in 2010 at the University of Adelaide. He joined the Institute for Photonics and Advanced Sensing as a Research Assistant developing thulium-doped fibre lasers. In 2011 he became a PhD candidate within the Department of Physics researching MCVD fabrication, novel waveguide structures and high power fibre laser devices.

David G. Lancaster completed a BSc in science (physics, Hons 1) at the University of NSW, Sydney, Australia, 1991; And was awarded a PhD in laser physics from Macquarie University, Sydney (1997).
He spent three years as a Postdoctoral Fellow at Rice University, Houston, Texas, USA, developing difference frequency based mid-infrared spectrometers for high sensitivity molecular spectroscopy. He then worked for 10 years as a Snr Research Scientist at the Australian Defence Science and Technology Organisation, developing laser based countermeasure systems. In 2010 he moved to University of Adelaide where he established new activities in fiber fabrication, fiber and waveguide lasers. In 2015 he moved to the University of South Australia to establish the Laser Physics and Photonic Devices Laboratory.
Professor Lancaster is a member of the Australian Institute of Physics.

Peter C. Henry worked for 30 years as a Scientific Glass Blower for the University of Technology Sydney, The Commonwealth Scientific and Industrial Research Organisation and the University of New England. In 2001 he became an Optical Fibre Fabricator at Nufern and later at the Optical Fibre Technology Centre, for the University of Sydney. In 2010 he moved to the University of Adelaide to setup and operate the silica preform and fibre fabrication facilities for the Institute for Photonics and Advanced Sensing. In 2014 he founded MG Scientific Glassblowing in Sydney, New South Wales.

Tanya M. Monro was born in Sydney, Australia in 1973. She received the Ph.D., and BSc degrees in physics from The University of Sydney, New South Wales, Australia in 1998 and 1994 respectively.

In 2014, she joined the University of South Australia as the Deputy Vice Chancellor & Vice President: Research and Innovation and is an ARC Georgina Sweet Laureate. In 2005 she was appointed the inaugural Chair of Photonics at the University of Adelaide. Her main areas of research include novel optical fibres and nanophotonic approaches for sensing applications and has published over 500 papers in refereed journals and conference proceedings.

Prof. Monro is a member of the Prime Minister's Commonwealth Science Council, the Australian Academy of Science Committee for Physics, the South Australian Economic Development Board and a member of South Australia's Riverbank Authority. She was the recipient of the Eureka Prize for Excellence in Interdisciplinary Scientific Research in 2015, awarded the Beattie Steel Medal of the Australian Optical Society in 2014, and the Australian Academy of Sciences' Pawsey Medal in 2012. She was named South Australia's "Australian of the Year" and the Scopus Young Researcher of the Year in 2011. She became South Australian Scientist of the Year and Telstra Business Women of the Year (in the Community & Government category) in 2010, won the Prime Minister's Malcolm McIntosh Prize for Physical Scientist of the Year in 2008.

David J. Ottaway received his PhD degree from The University of Adelaide in 1999. His doctoral dissertation was on solid state laser sources for gravitational wave detection. In 2000 he joined the LIGO Laboratory, first as a postdoctoral scholar at the LIGO Hanford Observatory, Richland, Washington and later as a staff scientist at the Massachusetts Institute of Technology. During this period he conducted research on commissioning the Initial LIGO detectors and developing optical and mechanical systems for the Advanced LIGO detectors. In 2007 he joined the staff at The University of Adelaide where he continues to develop laser and optical systems for advanced gravitational wave detectors and other forms of extreme remote sensing including remote trace gas detection and atmospheric temperature studies.